—Original—

Critical Roles of Capillary Endothelial Cells for Alveolar Remodeling in Nonspecific and Usual Interstitial Pneumonias

Akitoshi Tachihara[1,2], Enjing Jin[1], Toshiaki Matsuoka[1,2], Mohammad Ghazizadeh[1],
Shinichi Yoshino[2], Tamiko Takemura[3], William D. Travis[4] and Oichi Kawanami[1]

[1]Department of Molecular Pathology, Institute of Gerontology, Nippon Medical School, Graduate School of Medicine
[2]Department of Joint Disease and Rheumatism, Nippon Medical School, Graduate School of Medicine
[3]Department of Surgical Pathology, Japan Red Cross Hospital Center
[4]Department of Pathology, Memorial Sloan-Kettering Cancer Center, USA

Abstract

To characterize the relationship between angiogenesis factors and alveolar remodeling in interstitial lung diseases, we examined alveolar capillary endothelial cells in the normal lung (n=5) and in lungs with nonspecific interstitial pneumonia (NSIP) (n=4) or usual interstitial pneumonia (UIP) (n=6) using immunofluorescence staining for thrombmodulin and von Willebrand factor (vWF). With three-dimensional images of alveolar capillaries, the diameter of capillary tubes and their branching frequency per unit length were determined to define rearrangement of the capillary meshwork. Alveolar capillary endothelial cells in normal lungs expressed surface thrombomodulin, and those in lungs with cellular NSIP often showed coexpression of surface thrombmodulin and cytoplasmic vWF. In the alveolar septa of fibrotic NSIP and UIP, capillary endothelial cells demonstrated vWF in only the cytoplasm. Capillary branching frequencies in NSIP and UIP were decreased to 45% and 22%, respectively, of the normal level ($p<0.002$). Compared with normal lungs, in NSIP and UIP lungs alveolar capillaries containing TUNEL-positive endothelial cells ($p<0.05$) showed increases of 3.6-fold and 4.3-fold, respectively, indicating a close correlation between endothelial cell apoptosis and remodeling of alveolar capillary frameworks. The analysis of mRNA expression of vascular endothelial growth factors (VEGF) and their receptors (VEGFR1 and VEGFR2) showed a significant decrease in each VEGF isoform and in VEGFR2 mRNA in representative alveolar wall tissues microdissected from the normal, NSIP, and UIP lungs. These results suggest that decreased expression of VEGF mRNA is associated with a reduction in the number of capillary tubes via endothelial cell apoptosis that possibly results in alveolar remodeling in NSIP and UIP. However, whether VEGF is related to fibroblastic activation in the interstitial matrix remains unclear.
(J Nippon Med Sch 2006; 73: 203–213)

Key words: capillary endothelium, alveolar capillary remodeling, interstitial pneumonia, nonspecific interstitial pneumonia, usual interstitial pneumonia

Introduction

Most patients with idiopathic interstitial lung disease have earlier been diagnosed as having idiopathic pulmonary fibrosis or cryptogenic fibrosing alveolitis. They were then divided into two large sub-groups, such as usual interstitial pneumonia (UIP) and nonspecific interstitial pneumonia (NSIP)[1,2]. Additional, less common, categories include desquamated interstitial pneumonia (DIP), cryptogenic organizing pneumonia (COP), respiratory bronchiolitis with interstitial lung disease (RB-ILD), and acute interstitial pneumonia (AIP)[1].

UIP is histologically characterized by a temporally and spatially heterogeneous pattern of ongoing lung injury leading to the formation of fibroblastic foci (small aggregates of actively proliferating fibroblasts or myofibroblasts) adjacent to established alveolar fibrosis. However, it is in dispute whether the earliest stimuli to induce fibroblastic foci in alveolar structure involve alveolar inflammation. Histological features of UIP are hardly indicative of new capillary formation in the alveolar walls, but limited proliferation of microvessels has been observed adjacent to fibroblastic foci[3]. In contrast, NSIP lesions generally show homogeneous changes of predominantly inflammatory reaction (cellular NSIP) or mostly fibrotic change (fibrotic NSIP) in alveolar structures. In cellular NSIP, alveolar capillaries are often intermingled with inflammatory cells, whereas NSIP in fibrotic type appears to contain fewer capillaries.

Capillaries might play important roles in inducing morphological alteration in alveolar structures. Evidence for possible roles are that capillary sprouting and fibroblast proliferation characterize early pathological changes of granulation tissue during wound healing and that in the later stage capillary number decreases considerably while collagen fiber densely accumulates in the matrix to form what is described as fibrosis or scar. In this process the number of capillaries decreases through endothelial cell apoptosis.

On the other hand, the coagulation cascade has recently been considered to be intimately involved in the induction of alveolar fibrosis[4-6]. Thrombin plays major roles in converting fibroblasts into activated myofibroblasts and inducing their proliferation with collagen deposition in the matrix[7]. Thrombomodulin, a thrombin receptor, is consistently expressed along the surfaces of alveolar capillary endothelial cells and exerts a protective effect against blood coagulation[8] that is regulated by VEGF[9]. Upon formation of the thrombin-thrombomodulin complex, protein C is activated to inhibit further generation of thrombin and related coagulation factors[10]. Loss of endothelial surface thrombomodulin often occurs under acute inflammation[11] or extension of neoplastic cells of lung adenocarcinoma along alveolar wall linings[12]. The alveolar endothelial cells, in turn, express new surface antigens[13,14]. Whereas thrombomodulin expression is lost, cytoplasmic vWF often occurs in association with alveolar fibrosis in human interstitial pneumonia and in experimental silicosis[15]. These phenotypic changes of endothelial cells suggest functional alterations that have various effects on surrounding cells and the microenvironment. To characterize the relationship between angiogenesis factors and alveolar remodeling in interstitial lung diseases, in this study we examined alveolar capillary endothelial cells in the normal lung and in lungs with NSIP or UIP.

Materials and Methods

Patients

Control lung tissues were obtained from histologically normal areas of lung lobes removed to treat isolated benign tumors (n=5, 2 men and 3 women, all nonsmokers, average age, 55.1 years). Open lung biopsies were performed in 4 patients with NSIP (n=4, 1 man and 3 women; average age, 53.0 years). One male patient was a smoker (94 pack-years) and showed a NSIP fibrotic pattern, and the other 3 nonsmokers showed a cellular pattern. The patients with UIP (6 men; average age, 61.7 years) were all smokers (6 to 95 pack-years). Most patients had not received any treatment before biopsy, except one UIP patient who had once received

predonisolone. The diagnoses of these patients were established on the basis of the criteria of the American Thoracic Society/European Respiratory Society Consensus Classification[1]. This study was approved by the Ethical Committee Associations of Japan Red Cross Center Hospital and of Nippon Medical School.

Histological Examination

Biopsy specimens were divided into 2 pieces. One part was fixed in 10% buffered formalin for 2 days, dehydrated, and embedded in paraffin. Serial sections were stained with hematoxylin and eosin (H&E) or used for immunostaining as described below. The remaining part was freshly embedded in OCT compound, snap frozen in acetone dry ice, and stored at −80℃ until use. Fresh-frozen sections were used for microdissection of alveolar wall tissues representing normal, NSIP, or UIP lungs, as described previously[8,12–14], for analysis of mRNA expression. Frozen sections were also used for indirect dual immunofluorescence staining.

Dual Immunofluorescence Staining

Dual immunofluorescence staining was done as described in our previous report[8,12–14]. Briefly, frozen sections were incubated overnight at 4℃ with a combination of a mouse monoclonal IgG antibody against thrombomodulin (1:50 dilution) (TM1009; DAKO, Carpinteria, CA, USA) and a rabbit polyclonal antibody against vWF (1:400 dilution; DAKO, Glostrup, Denmark) as the two primary antibodies. Specimens were treated with a mixture of the 2 secondary antibodies: 1:100 dilutions of Texas Red-labeled horse anti-mouse immunoglobulin G (IgG) and fluorescein isothiocyanate (FITC)-labeled goat anti-rabbit IgG (Vector Laboratories , Burlingame, CA, USA), for 40 min at room temperature in the dark. Nuclear counterstaining was performed for 15 min at room temperature with 0.01% TOTO-3 iodide (Molecular Probes, Eugene, OR, USA). The sections were observed under a confocal laser scanning microscope (model TC-SP, Leica, Heidelberg, Germany) equipped with argon and argon-krypton laser sources. Red fluorescence represented thrombomodulin , and green fluorescence represented vWF.

The Diameter and Branching Frequency of Alveolar Capillaries

The diameters of alveolar capillaries were measured. Because the counting of capillaries per unit area of histological specimens is unreliable owing to the inconsistency of air spaces that depend on the fixation conditions of lung tissue, we focused instead on the branching frequency. To accurately evaluate possible remodeling in the capillary meshwork of the alveolar walls, we measured the branching frequency of capillaries in approximately 30-μm-thick frozen sections by estimating the length between 2 openings of adjacent capillary tube branches.

Immunohistochemical Staining for Caspase 3 (Active Form)

Avidin-biotin complex immunostaining was used to identify the active form of caspase 3 (rabbit polyclonal IgG, Abcam Limited, Cambridgeshire, UK). The sections were pretreated with proteinase K (20 μg/ml) for 30 min at 37℃, after which endogenous peroxidase was inhibited. The primary antibody for caspase 3 was applied for 1 hr at 37℃. Biotin-labeled goat anti-rabbit IgG was used as the secondary antibody, and the chromogenic reaction was performed with diaminobenzidine (DAB).

Immunofluorescence and Immunohistochemical Control Procedures

Negative control preparations consisted of 1) omission of the primary antibody from the staining procedure and 2) corresponding amounts of normal immunoglobulin for the primary antibodies. Both control procedures gave negative results.

Terminal Deoxynucleotidyl Transferase-mediated Deoxyuridine Triphosphate-biotin Nick-end Labeling Assay

For the terminal deoxynucleotidyl transferase-mediated deoxyuridine triphosphate-biotin nick-end labeling (TUNEL) assay, an in-situ cell death detection kit (POD) was applied (Roche Diagnostics GmbH, Mannheim, Germany) to paraffin-embedded

sections according to the manufacturer's instructions. The reaction product in nuclei was developed with DAB.

Apoptotic Tendency of Alveolar Capillary Endothelial Cells

An average of 36 alveolar wall capillary areas were observed in the normal and pathologic lung tissues under a middle-power field. We considered microvessels to be positive when more than one endothelial cell cytoplasm or their nuclei were reactive for caspase 3 staining or TUNEL method in one microvessel loop.

Reverse Transcription-polymerase Chain Reaction

The reverse transcription-polymerase chain reaction (RT-PCR) procedure used has been described previously[8,11–13]. Briefly, total RNA was extracted with an RNeasy Mini Kit (Qiagen, Hilden, Germany) from microdissected alveolar wall tissues and from the normal and representative alveolar walls of patients with NSIP or UIP. Complementary (c) DNA was synthesized from total RNA primed with oligo (dT) using superscript II reverse transcriptase (Gibco BRL) at 42℃ for 1 hr. RT-PCR was performed with 1 μl of cDNA products.

For VEGF, VEGFR2, and VEGFR1 mRNA expression, RT-PCR was performed with primers that span the variable splice regions of VEGF mRNA: (a) 5'-GCT ACT GCC ATC CAA TCG AGA CC-3' (sense) and (b) 5'-GTT TCT GGA TTA AGG ACT GTT CTG TCG-3' (anti-sense). The amplification was carried out using 0.4 mol/L of each primer for 40 cycles (1 min at 94℃, 1 min at 60℃, and 2 min at 72℃). The PCR products for each VEGF variant of 440, 572, 644, and 695 base-pairs (bp) encode the isoforms of $VEGF_{121}$, $VEGF_{165}$, $VEGF_{189}$, and $VEGF_{206}$, respectively. For VEGFR2, PCR was performed with the primers 5'-CAT CAC ATC CAC TGG TAT TGG C-3' (sense) and 5'-GGC CAA GCT TGT ACC ATG TGA G-3' (anti-sense) for 40 cycles (45 sec at 94℃, 45 sec at 56℃, and 2 min at 72℃), for a fragment size of 403 bp. For VEGFR1, PCR was performed with the primers 5'-GCA AGG TGT GAC TTT TGT TCC-3' (sense) and 5'-GAG

GAT TTC TTC CCC TGT GTA-3' (anti-sense) for 40 cycles (45 sec at 94℃, 45 sec at 61℃, and 2 min at 72℃), with an amplified product of 512 bp. The PCR products were electrophoresed on 2% agarose gels and visualized with ethidium bromide staining. Glyceraldehyde 3-phosphate dehydrogenase (GAPDH) was used as an internal control. Semiquantitative measurements were performed on the basis of standard curves constructed for the products and GAPDH. The analyses were performed using Quantity One Quantification Software (Bio-Rad Laboratories, Hercules, CA, USA).

Statistical Analysis

All values are expressed as means ± SE. Significance was determined with a one-way analysis of variance with the Student-Newman-Keuls test to determine differences among groups. These tests were performed with SPSS statistical software (SPSS, Inc., Chicago, IL, USA), and p values of less than 0.05 or 0.01 were considered to indicate significance.

Results

Histological Findings

The normal alveolar capillaries occupied most areas of the alveolar wall structure (H&E; **Fig. 1A**). A small number of elastic fibers and smooth muscle cells were located mainly in the alveolar ducts. Of 4 patients with NSIP, 3 patients had a cellular pattern, and 1 had a fibrotic pattern. In the cellular pattern of NSIP, a large number of mononuclear cells consistently occupied the interstitial matrix of alveolar walls (**Fig. 1B**). A fibrin-rich exudate was occasionally found in air spaces and was often enclosed by extensions of epithelial cells (organizing pneumonia) (**Fig. 1B**). Most alveolar walls in the cellular pattern appeared quite enlarged with edema and inflammatory cells. Alveolar capillary lumens often tended to be collapsed, whereas the general architecture was retained to various degrees. In the fibrotic pattern of NSIP, the alveolar walls were characterized by uniform collagen deposition without fibroblastic foci (**Fig. 1C**). In each patient with UIP, fibroblastic foci had developed subjacent
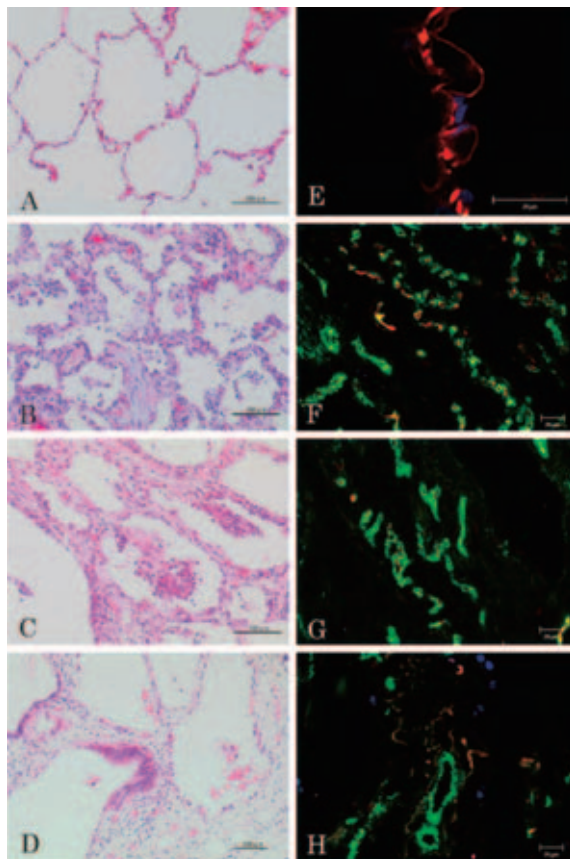
A, E: Normal lung

B, F: NSIP (Cellular pattern)

C, G: NSIP (Fibrotic pattern)

D, H: UIP

Fig. 1 **A ~ D** (Bar = 100 μm.) Histological features of normal (A), NSIP (B and C), and UIP (D) lungs. H&E stain.

1A: Normal alveolar structure consists of a scant amount of connective tissue matrix and a fine capillary network.

1B: Alveolar architecture is relatively well perserved (cellular pattern) with infiltration of numerous mononuclear cells and slight to mild edema or collagen deposition. Intra-alveolar organization is clearly seen at the center bottom of the micrograph.

1C: Alveolar walls are thickened with moderate collagen deposition. Fewer inflammatory cells are scattered in the walls, but macrophages are still abundant in the lumens.

1D: Alveolar walls demonstrate varying degrees of thickening with collagen that is covered by regenerating epithelial cells. At the center of the micrograph the alveolar wall is covered by bronchiolar epithelial cells (bronchiolar metaplasia).

E ~ H: Dual immunofluorescence study with Texas red-labeled thrombomodulin (red) and FITC-labeled vWF (green). Nuclei are stained with TOTO-3 (blue).

1E: The normal alveolar capillaries show thrombomodulin expression along the endothelial cell surfaces. No vWF is seen along the capillaries.

1F: Capillaries in alveolar walls with cellular pattern of NSIP are characterized by thrombomodulin expression at the inner surface of endothelial cells surrounded by cytoplasmic vWF. The cross section of alveolar capillary endothelial cells show a toroidal pattern.

1G: In the fibrotic pattern of NSIP, alveolar capillaries are located along the central axis of thickened alveolar walls. The endothelial cell cytoplasm expresses vWF alone.

1H: The capillary network is simplified in alveolar walls with a large amount of collagen deposition and elastic fibers. Capillaries are often located along the central axis of the walls and are engorged in some places and collapsed in others.

to patchy fibrotic scars. Capillaries were hardly recognizable in the fibrotic alveolar walls, but the connective tissue matrix of alveolar walls located immediately adjacent to fibroblastic foci contained widely opened microvessels. Five of 6 patients with UIP demonstrated honeycombing, and bronchiolar metaplasia was present within or near the honeycomb lesions **(Fig. 1D)**. The alveolar capillaries in honeycombing were collapsed. Despite the presence of marked fibrosis in UIP, the areas of relatively uninvolved lung contained a normal alveolar framework with intact capillaries as well. No particular characteristics were found in the

patient treated with predonisolone.

Immunofluorescence Observations of Alveolar Capillary Endothelial Cells

Confocal microscopic examination revealed linear expression of thrombomodulin along the surfaces of normal alveolar capillary endothelial cells **(Fig. 1E)**. However, vWF was not expressed in the cytoplasm of these cells **(Fig. 1E)**.

In areas of the cellular pattern in NSIP, thrombomodulin expression was partly lost along the surfaces of endothelial cells in each patient but was fairly well retained in the adjacent alveolar
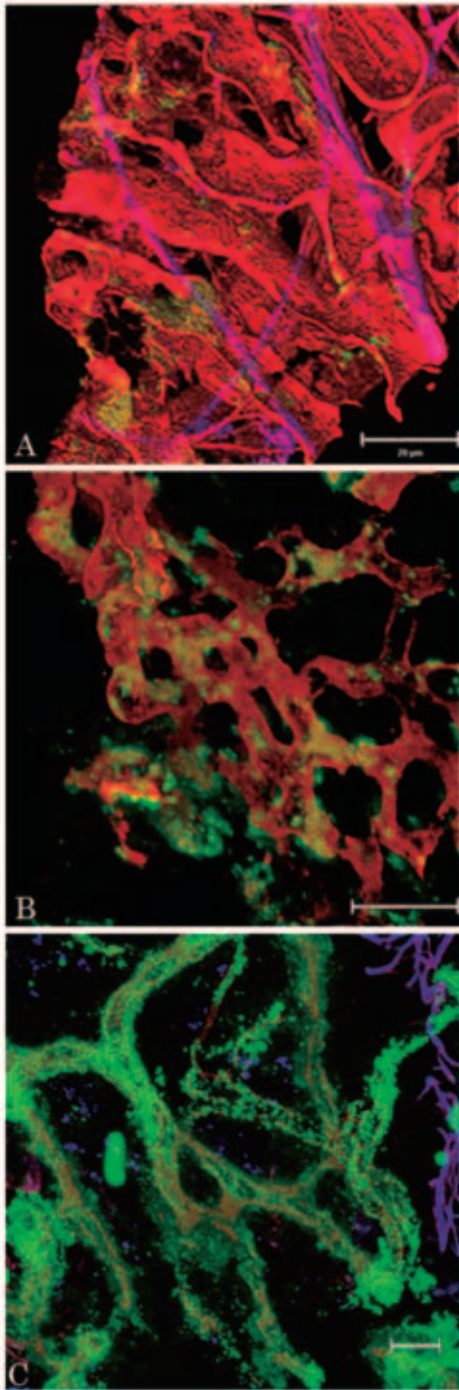
A: Normal lung

B: NSIP (Cellular pattern)

C: UIP

Fig. 2　Three-dimensional images of dual immunofluorescence staining depicting Texas Red-labeled thrombomodulin and FITC-labeled vWF in normal (2A), NSIP (2B), and UIP (2C) lungs.

zone. Moreover, vWF was frequently coexpressed in the same segments of alveolar capillary endothelial cells. Cross sections of capillaries clearly demonstrated a toroidal staining pattern consisting of the inner Texas Red (thrombomodulin) and the outer FITC green colors (vWF) **(Fig. 1F)**. In relation to smoking, no differences in immunohistochemical expression were found, although only one patient in the NSIP group smoked. The intensity of cytoplasmic staining for vWF increased in proportion to the degree of collagen deposition in alveolar fibrosis of NSIP and UIP **(Fig. 1G)**. In UIP, alveolar capillaries located in the thick connective tissue matrix immediately adjacent to fibroblastic foci were often widely dilated and undulated. Their endothelial cells were exclusively reactive for vWF but were unreactive for thrombomodulin **(Fig. 1H)**. Most fibroblastic foci contained no capillaries, although only small aggregations of cytoplasmic segments reactive for vWF were found in 2 patients.

To sufficiently reveal the capillary meshwork in the mural structure of alveolar walls, the confocal microscopic observations were made through 30-μm-thick layers of frozen tissue sections. The surfaces of normal alveolar capillary endothelial cells were completely covered by thrombomodulin, and the cytoplasm did not express vWF **(Fig. 2A)** at all. In the cellular pattern of NSIP, alveolar capillaries were surrounded with irregular and edematous boundaries that were positive for vWF. A vWF-positive cytoplasm was also discernible, separated by cell membranes reactive for thrombomodulin **(Fig. 2B)**. In the fibrotic pattern of NSIP and in fibrotic areas of UIP, the capillary meshwork became much looser and undulated with a reduced frequency of branching. The cell membranes of alveolar capillary endothelial cells became unreactive for thrombomodulin. Instead, the cytoplasm of alveolar capillary endothelial cells was fully reactive for vWF **(Fig. 2C)**.

The Diameter and Branching Frequency of Alveolar Capillaries

The average diameters of capillary tubes were 7.0 ± 0.3 μm in normal lungs, 6.0 ± 0.2 μm in NSIP lungs, and 8.8 ± 0.6 μm in UIP lungs **(Fig. 3A)**. The
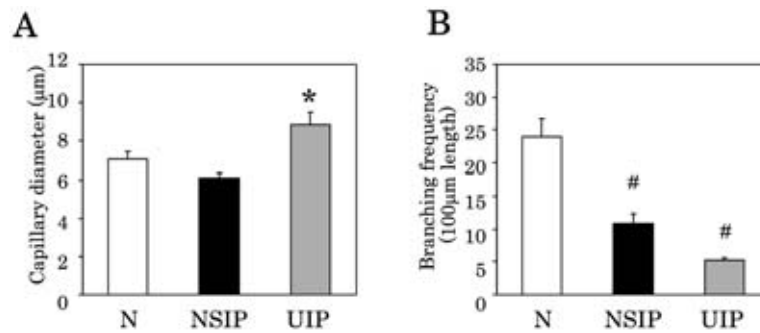
Fig. 3   Average diameters of alveolar capillaries of normal (N), NSIP, and UIP lungs in **3A**. The branching frequency per 100 μm is derived from the average length between the neighboring branches in capillary anastomoses (3B).
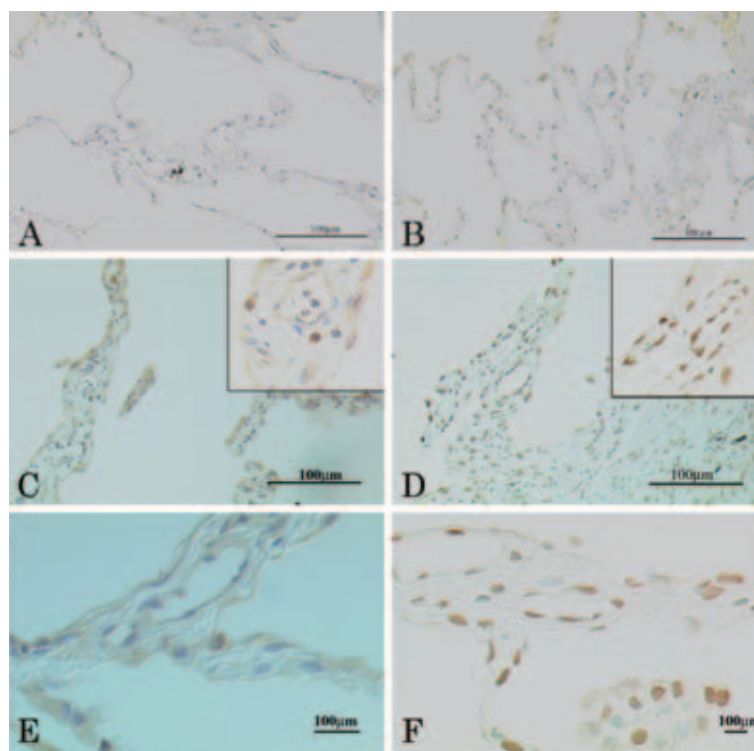

Fig. 4   Immunohistochemical staining for caspase 3 (active form) (4A, 4C and 4E), and the TUNEL assay (4B, 4D and 4F). Compared with those in normal lungs, both reactions in the interstitial pneumonias were significantly increased (p<0.05). Both reactions were significantly lower in NSIP lungs than in UIP lungs (p<0.05). The reactions of capillaries indicated by an arrow in the original pictures were inserted in the right upper corners of Figures 4C ～ 4F. The magnification of each insert was 2-fold higher than the original picture.

distances between 2 entrances of neighboring tubes was significantly greater in NSIP and UIP than in normal lungs; thus, the mean numbers of branches per 100 μm were 24.0 ± 2.7, 10.9 ± 1.2, and 5.2 ± 0.3 in the normal, NSIP, and UIP lungs, respectively **(Fig. 3B)**.
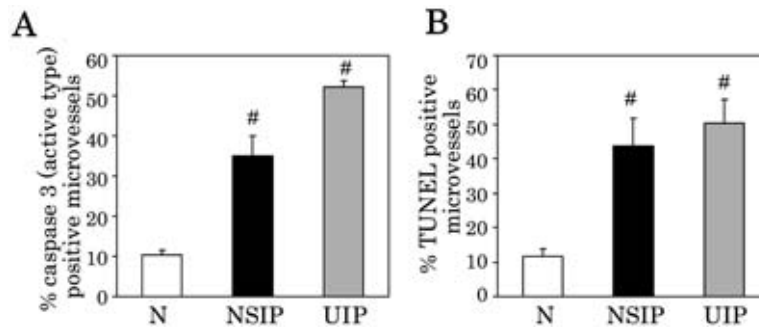
Fig. 5　Percentage of alveolar capillaries with endothelial cells positive for
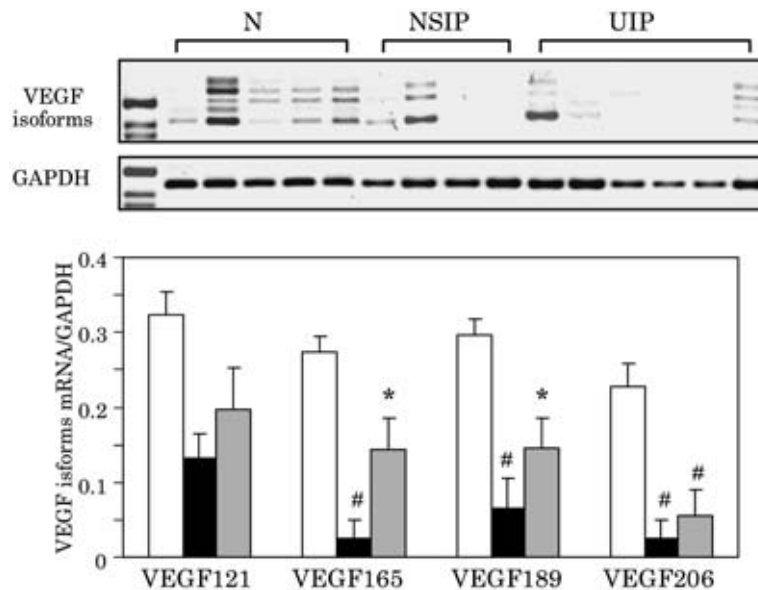caspase 3 (5A) and TUNEL (5B).

Fig. 6　Expression of VEGF isoform mRNA in the normal, RA, NSIP, and
UIP alveolar walls. Expression of each VEGF isoform was highest
in normal alveolar walls.

Apoptosis of Alveolar Capillary Endothelial Cells: Caspase 3 (Active Form) Reaction and TUNEL Analysis

In the normal alveolar structures, cells such as epithelial cells, capillary endothelial cells, interstitial fibroblasts, and macrophages were rarely reactive for caspase 3 (**Fig. 4A**). In contrast, caspase 3 reactions occurred diffusely in a variety of alveolar cells, especially in the epithelial and endothelial cells of both NSIP (**Fig. 4C**: capillaries in insert ×2) and UIP lungs (**Fig. 4E**: capillaries in insert ×2). In the alveolar walls, the rate of caspase 3-positive capillaries was $35.0 \pm 5.1\%$ in NSIP lungs, $52.2 \pm 1.5\%$ in UIP lungs ($p<0.05$), and $10.4 \pm 1.2\%$ in normal lungs. Thus, caspase 3-positive capillaries were more

frequent in NSIP lungs and UIP lungs ($p<0.05$) (**Fig. 5A**) than in normal lungs.

With the TUNEL assay, the reactivity of alveolar epithelial cells was minimal in normal lungs (**Fig. 4 B**), random in NSIP lungs (**Fig. 4D**), and most frequent in UIP lungs (**Fig. 4F**). The rate of TUNEL-positive cells located in alveolar walls was significantly higher in NSIP lungs ($42.2 \pm 6.44\%$) and UIP lungs ($50.2 \pm 6.90\%$) than in normal lungs ($11.7 \pm 2.11\%$) ($p<0.01$) (**Fig. 4B, 4D, and, 4F**), and the positive rate was significantly higher in UIP lungs than in NSIP lungs ($p<0.05$) (**Fig. 5B**).
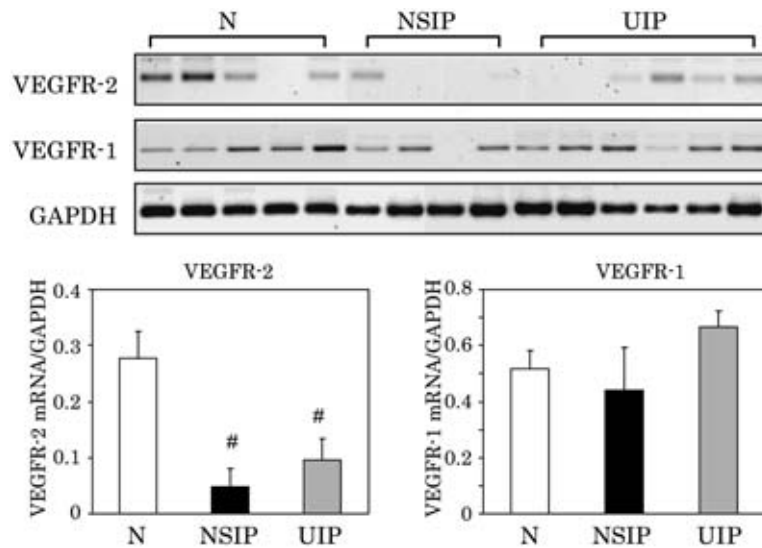
Fig. 7 Expression of VEGFR2 (left) and VEGFR1 (right) mRNA. The normal alveolar walls showed the highest expression of VEGFR2 mRNA. VEGFR2 mRNA expression was similar in UIP and in normal walls and was lowest in NSIP. There were no significant differences in the expression of VEGFR1 mRNA.

Expression of VEGF and VEGFR mRNAs in Microdissected Alveolar Wall Tissues

RT-PCR analysis demonstrated that the expression of each mRNA isoform (VEGF$_{121}$, VEGF$_{165}$, VEGF$_{189}$, and VEGF$_{206}$) was the highest in normal alveolar wall tissues (**Fig. 6**). The expression of VEGF$_{165}$, VEGF$_{189}$, and VEGF$_{206}$ mRNAs was significantly lower in NSIP lungs ($p<0.05$) and UIP lungs ($p<0.05$) than in normal lungs. The VEGF$_{165}$ mRNA expression in NSIP lungs was significantly lower ($p<0.05$) than in UIP lungs. The expression of VEGFR2 mRNA was significantly higher in the normal alveolar wall than in NSIP lungs ($p<0.05$) or UIP lungs ($p<0.01$). The VEGFR1 mRNA expression varied to some extent, but there were no significant differences among the normal lungs and lungs with interstitial pneumonias (**Fig. 7**).

Discussion

The present study using dual immunofluorescence staining has shown a series of phenotypic patterns in alveolar capillary endothelial cells in normal lungs and in lungs with interstitial pneumonias. Surface thrombomodulin was consistently expressed along the surface of normal capillary endothelial cells, as revealed previously[8,12–14]. The expression of thrombomodulin is believed to exert an anticoagulant effect by activating protein C as a consequence of thrombin-thrombomodulin complex formation[10]. This mechanism plays an important role in the maintenance of physiological circulation when pulmonary blood pressure is low.

In cellular NSIP, surface thrombomodulin was frequently coexpressed with cytoplasmic vWF in the same segments of endothelial cells of alveolar capillaries. According to Conway et al.[6], proinflammatory cytokines, such as tumor necrosis factor-α and interleukin-1β, induce an immediate loss of thrombomodulin, as found in endotoxin-treated animals[11,17]. Retention of thrombomodulin in cellular NSIP, which is histologically characterized by active inflammatory reaction, might be related to a lack of immediate release of participating proinflammatory cytokines, to partial suppression of such cytokine products, or to some other unknown causes that lead to a pathological loss of surface thrombomodulin.

In the present study, increases in cytoplasmic vWF in capillary endothelial cells were consistently found in fibrotic NSIP and UIP. This finding agrees well with our previous studies that demonstrated overexpression of vWF in alveolar capillary endothelial cells. Overexpression of vWF has been

shown by immunohistochemical and electron microscopic observations[15,18] during the development of alveolar fibrosis[18], experimental silicosis[15], and primary lung adenocarcinoma[12–14]. Direct causes of the phenotypic transformation of capillary endothelial cells remain unclear, as is the mechanism of the mosaic expression pattern of endothelial cells in the border zones between alveolar capillaries and adjacent microvessels[8].

The expression of vWF along capillary tubes in cellular NSIP is caused in part by exudation of vWF-positive serum components adherent to endothelium, because H&E staining of the alveolar interstitial matrix revealed swelling by edema fluid (**Fig. 1B and C**).

Increased levels of lymphocytes among the inflammatory cells recovered in bronchoalveolar lavage fluid (BALF) are found only in patients with NSIP[2]. In contrast, lymphocyte ratios in BALF from UIP patients are quite low, and larger numbers of macrophages, neutrophils and eosinophils are common. The prognosis of NSIP is generally better than that of UIP, which can be rapidly fatal. Relative retention of thrombomodulin expression suggests less severe involvement of alveolar capillary endothelial cells in cellular NSIP.

In the process of wound healing, mesenchymal cells, such as capillary endothelial cells and fibroblasts, are increased in the early stage, after which capillaries decrease in number and fibroblasts become activated to develop scar tissue with abundant collagen deposition. In this context, we focused on the number of alveolar capillaries and their meshwork pattern in alveolar walls in cellular/fibrotic NSIP and UIP. The tubular network of capillaries consists of full patchworks of endothelial cell along the inner surface of tubes. Insufficient recruitment of vascular endothelial cells should result in defects of the meshwork, leading to remodeling of the alveolar capillary structure. The average distance between adjacent capillary branches was the least in the normal alveolar walls. In other words, the branching frequency per unit length of capillaries was the highest in normal lungs, accurately indicating the losses of capillary branches in NSIP and UIP. Loss of capillaries may depend on

apoptotic death of endothelial cells.

The percentage of alveolar capillaries containing TUNEL-positive endothelial cells reached 42.2% in NSIP lungs and 50.2% in UIP lungs but was only 11.7% in normal lungs. Vascular endothelial apoptosis is closely related to VEGF/VEGFR expression in endothelial cells, and epithelial apoptosis plays an interesting role in fibrotic lung disease[19,20]. Because of the technical difficulty of separating cell types in alveolar walls, we analyzed mRNA expression in alveolar wall tissue with the microdissection method. The expression of $VEGF_{121}$, $VEGF_{165}$, $VEGF_{189}$, and $VEGF_{206}$ and VEGFR2 mRNA in the present study was higher in normal alveolar wall tissues than in NSIP and UIP lungs. VEGFs are believed to contribute to cell renewal and to the suppression of apoptotic activity in alveolar capillary endothelial cells to maintain alveolar structure and function. Kasahara *et al.*[21] have proved that lower levels of VEGF and VEGFR2 proteins are closely related to emphysemtous reconstruction of the alveolar component. They have also experimentally induced emphysema-like lung structures in rats by means of the VEGFR2 inhibitor SU5416. Such lung remodeling has also been produced by Tang et al.[22] in transgenic VEGF*loxP* mice by VEGF gene ablation targeted to the lung. Thus, an imbalance of the pulmonary VEGF and VEGFR system leads to emphysema-like remodeling of the lung[23]. Our present results suggest that universal reduction of VEGF isoforms and VEGFR2 mRNA expression induces alveolar capillary endothelial cell apoptosis. As a result, alveolar capillaries are regressed, producing defects in the capillary meshwork resulting in alveolar structural remodeling, as in NSIP and UIP. However, in the present study we could not determine whether collagen deposition in alveolar walls is also due to an imbalance of VEGF and VEGFR expressions in NSIP and UIP.

On the other hand, the alveolar walls in UIP demonstrated higher VEGF mRNA expression than did those in NSIP. Ebina et al.[3] have demonstrated possible heterogeneous angiogenic capacity in UIP lungs with three-dimensional reconstruction . However, their results did not reveal any functional aspects of alveolar capillary endothelial cells with

regard to apoptosis. Our present results clearly indicate that differences in VEGF/VEGFR mRNAs expression among normal, NSIP, and UIP lungs which might contribute to the induction of apoptosis in capillary endothelial cells.

In conclusion, the physiological functions and structure of normal alveolar capillaries are maintained under the strict regulation with relatively high expression of VEGF/VEGFR mRNA. Our data suggest that a significant reduction in VEGF/VEGFR mRNA in alveolar walls plays a fundamental role in the induction of structural remodeling in NSIP and UIP via an imbalance between recruitment and apoptosis of capillary endothelial cells. The role of VEGF in interstitial fibrosis remains unclear.

References

1. The ERS Executive Committee, 2002. American Thoracic Society/European Respiratory Society International Multidisciplinary Consensus Classification of the Idiopathic Interstitial Pneumonias: This joint statement of the American Thoracic Society (ATS), and the European Respiratory Society (ERS) was adopted by the ATS board of directors. Am J Respir Crit Care Med 2002; 165: 277–304.

2. Nagai S, Kitaichi M, Itoh H, Nishimura K, Izumi T, Colby TV: Idiopathic nonspecific interstitial pneumonia/fibrosis: comparison with idiopathic pulmonary fibrosis and BOOP. Eur Respir J 1998; 12: 1010–1019.

3. Ebina M, Shimizukawa M, Shibata N, et al.: Heterogeneous increase in CD34-positive alveolar capillaries in idiopathic pulmonary fibrosis. Am J Respir Crit Care Med 2004; 169: 1203–1208.

4. Chambers RC: Role of coagulation cascade proteases in lung repair and fibrosis. Eur Respir J Suppl 2003; 44: 33s–35s.

5. Yasui H, Gabazza EC, Tamaki S, et al.: Intratracheal administration of activated protein C inhibits bleomycin-induced lung fibrosis in the mouse. Am J Respir Crit Care Med 2001; 163: 1660–1668.

6. Shimizu S, Gabazza EC, Taguchi O, et al.: Activated protein C inhibits the expression of platelet-derived growth factor in the lung. Am J Respir Crit Care Med 2003; 167: 1416–1426.

7. Ludwicka-Bradley A, Bogatkevich G, Silver RM: Thrombin-mediated cellular events in pulmonary fibrosis associated with systemic sclerosis (scleroderma). Clin Exp Rheumatol 2004; 22: S38–S46.

8. Kawanami O, Jin E, Ghazizadeh M, et al.: Mosaic-like distribution of endothelial cell antigens in capillaries and juxta-alveolar microvessels in the normal human lung. Pathol Int 2000; 50: 136–141.

9. Calnek DS, Grinnell BW: Thrombomodulin-dependent anticoagulant activity is regulated by vascular endothelial growth factor. Exp Cell Res 1998; 238: 294–298.

10. Esmon CT: The protein C pathway. Chest 2003; 124: S26–S32.

11. Terada Y, Eguchi Y, Nosaka S, Toba T, Nakamura T, Shimizu Y: Capillary endothelial thrombomodulin expression and fibrin deposition in rats with continuous and bolus lipopolysaccharide administration. Lab Invest 2003; 83: 1165–1173.

12. Jin E, Fujiwara M, Nagashima M, et al.: Aerogenous spread of primary lung adenocarcinoma induces ultrastructural remodeling of the alveolar capillary endothelium. Hum Pathol 2001; 32: 1050–1058.

13. Jin E, Ghazizadeh M, Fujiwara M, et al.: Angiogenesis and phenotypic alteration of alveolar capillary endothelium in areas of neoplastic cell spread in primary lung adenocarcinoma. Pathol Int 2001; 51: 691–700.

14. Jin E, Fujiwara M, Pan X, et al.: Protease-activated receptor (PAR)-1 and PAR-2 participate in the cell growth of alveolar capillary endothelium in primary lung adenocarcinomas. Cancer 2003; 97: 703–710.

15. Kawanami O, Jiang HX, Mochimaru H, et al.: Alveolar fibrosis and capillary alteration in experimental pulmonary silicosis in rats. Am J Respir Crit Care Med 1995; 151: 1946–1955.

16. Conway EM, Rosenberg RD: Tumor necrosis factor suppresses transcription of the thrombomodulin gene in endothelial cells. Mol Cell Biol 1988; 8: 5588–5592.

17. Moore KL, Andreoli SP, Esmon NL, Esmon CT, Bang NU: Endotoxin enhances tissue factor and suppresses thrombomodulin expression of human vascular endothelium in vitro. J Clin Invest 1987; 79: 124–130.

18. Kawanami O, Matsuda K, Yoneyama H, Ferrans VJ, Crystal RG: Endothelial fenestration of the alveolar capillaries in interstitial fibrotic lung diseases. Acta Pathol Jpn 1992; 42: 177–184.

19. Kuwano K, Miyazaki H, Hagimoto N, et al.: The involvement of Fas-Fas ligand pathway in fibrosing lung diseases. Am J Respir Cell Mol Biol 1999; 20: 53–60.

20. Kuwano K, Hagimoto N, Maeyama T, et al.: Mitochondria-mediated apoptosis of lung epithelial cells in idiopathic interstitial pneumonias. Lab Invest 2002; 82: 1695–1706.

21. Kasahara Y, Tuder RM, Cool CD, Lynch DA, Flores SC, Voelkel NF: Endothelial cell death and decreased expression of vascular endothelial growth factor and vascular endothelial growth factor receptor 2 in emphysema. Am J Respir Crit Care Med 2001; 163: 737–744.

22. Tang K, Rossiter HB, Wagner PD, Breen EC: Lung-targeted VEGF inactivation leads to an emphysema phenotype in mice. J Appl Physiol 2004; 97: 1559–1566.

23. Kanazawa H, Hirata K, Yoshikawa J: Imbalance between vascular endothelial growth factor and endostatin in emphysema. Eur Respir J 2003; 22: 609–612.